

TEMPERATURE DISTRIBUTION INSIDE GTEM-CELL FOR BIOMEDICAL EXPERIMENTS

Šalovarda M.¹, Malarić K.², Malarić R.²

¹DEKOD telekom d.o.o., Horvacanska c. 17a/7 Zagreb, Croatia

²Department of Wireless Communications,
Faculty of Electrical Engineering and Computing (FER), Zagreb, Croatia

Abstract: This paper models temperature distribution inside a GTEM-cell. In testing biological effects of electromagnetic field it is necessary to dismiss the thermal effect. That is why it is necessary to see how and to what effect electromagnetic field increases the temperature inside the GTEM-cell.

Keywords: GTEM cell, temperature distribution

1. INTRODUCTION

The increasing use of technology in our everyday environment has led to the ubiquitous presence of electromagnetic fields. Such fields arise wherever there is voltage or current. All types of radio broadcasting and TV transmitters produce electromagnetic fields, and they also arise in industry, business and home, where they affect us even if our sense organs perceive nothing.

Generally we can divide biological effects of RF electromagnetic radiation into non-thermal and thermal effects. Non-thermal biological effects are related to LF EM field and are mostly manifested as induced currents in human body. Thermal biological effects happen due to HF EM field. Radio frequency radiation (RFR) interacts with matter by causing molecules to oscillate with the electric field. This interaction is most effective for polar molecules (that have their own internal electric field) such as water. A water molecule loses this rotational energy via friction with other molecules and causes an increase in temperature. This effect is the basis for microwave cooking. The RFR absorbed by the body occurs primarily as a result of the interaction with water.

The degree of absorption is a function of frequency and intensity of the field and the type of tissue. The depth of penetration decreases at higher frequencies.

Fields above 10 GHz are absorbed at the skin surface. Only a small portion of energy penetrates into the underlying tissue. Very high field strength is needed to produce cataracts or skin burns [1-4].

Related to human thermoregulation, organs with the least blood flow are most endangered. The eyes are particularly vulnerable to RF energy in the microwave range, and prolonged exposure to microwaves can lead to cataracts [5][6]. Each frequency in the electromagnetic spectrum is absorbed by living tissue at a different rate, called the specific absorption rate or SAR [3-6], (unit is watts per kilogram of tissue (W/kg)). The IEEE and many national governments have established safety

limits for exposure to various frequencies of electromagnetic energy based on SAR.

$$SAR = \frac{\sigma E^2}{\rho} \quad [1]$$

where E is the RMS value of the electric field strength in the tissue in V/m, σ is the conductivity of body tissue in S/m and ρ is density of body tissue in kg/m³.

2. THERMOREGULATION

Thermoregulation, which is part of the complex system involving circulation, metabolism, respiration and neural structures, can be divided into two components: a physiological component made up of heat production and heat loss mechanisms and a behavioral component that has sensory, motivational and response aspect. The mechanisms of heat regulation are activated by thermal receptors in the skin and direct stimulation of the hypothalamus by changes in blood temperature. Thermal receptors are distributed in a defined pattern in the skin. Much sensory summation occurs so that threshold for stimulation decreases as the size of the area stimulated increases.

Extensive investigations into microwave bioeffects during the last century indicate that, for frequencies between 200 and 24.5 GHz, exposure to a power density of 100mW/cm² or greater than 4mW/g for several minutes or hours can result in physiological manifestations of a thermal nature in laboratory animals [5-6].

Temperature increase during exposure to microwaves depends on: the specific area of the body exposed and the efficiency of heat elimination, field strength intensity, duration of exposure, specific frequency or wavelength; and thickness of skin and subcutaneous tissue. For instance fatty tissue has a considerably lower heat conductivity than muscular tissue. As a consequence the subcutaneous fat layer tends to establish a temperature barrier between inside and outside human body. Thermally the body is considered to be an inner core at the constant regulated temperature and an outer shell of variable temperature. In humans 2/3 of the body is at core temperature while 1/3 is at the shell temp [6].

In partial-body exposure under normal conditions, the body acts as a cooling reservoir, which stabilizes the temperature of exposed part. Heat transport is due to increase blood flow to cooler parts of the body, maintained at normal temperature by heat-regulating mechanisms such as heat loss due to evaporation, radiation and convection. If the amount of absorbed energy exceeds the optimal amount of heat energy that can be handled by mechanisms of temperature regulation, the excess energy will cause continuous temperature rise over time. Hyperthermia and local tissue destruction can result.

Many studies on animals have shown that RF irradiation that results in a rise of body core temperature to 43 or 44°C (109.4 or 111.2°F) from the normal 37°C (98.6°F) is lethal to the organism. However, the amount of energy that needs to be absorbed to achieve this temperature change is very large (over 100 mW/cm² for an extended period of time) , and would never be encountered by the public [5,6].

3. FINITE ELEMENT METHOD

The Finite element method is used to solve complex, nonlinear problems in electromagnetism [8-9]. The first step in finite-element analysis is to divide the analyzed configuration into small homogeneous elements. The model contains information about the device geometry, material constants, excitations and boundary constraints. In each finite element, a linear variation of the field quantity is assumed. The corners of the elements are called *nodes*. The goal is to determine the field quantities at the nodes.

The Finite-Element Analysis technique solves the unknown field quantities by minimizing the *energy functional*. *Energy functional* is an expression describing all the energy associated with the configuration being analyzed. For 3-dimensional, time-harmonic problems this functional may be represented as,

$$F = \int_v \frac{\mu |H|^2}{2} + \frac{\varepsilon |E|^2}{2} - \frac{J \cdot E}{2j\omega} dv \quad [2]$$

The first two terms in the integrand represent the energy stored in the magnetic and electric fields and the third term is the energy dissipated (or supplied) by the conduction currents.

By expressing H in terms of E and by setting the derivative of this functional with respect to E equal to zero, an equation of the form $f(J,E) = 0$ is obtained. A k th order approximation of the function f is then applied at each of the N nodes and the boundary conditions are enforced, resulting in the system of equations.

$$\begin{bmatrix} J_1 \\ J_2 \\ \cdot \\ \cdot \\ J_n \end{bmatrix} = \begin{bmatrix} y_{11} & y_{12} & \cdot \cdot \\ y_{21} & y_{22} & \cdot \cdot \\ \cdot \cdot \cdot \cdot \\ \cdot \cdot \cdot \cdot \\ \cdot \cdot \cdot y_m \end{bmatrix} \begin{bmatrix} E_1 \\ E_2 \\ \cdot \\ \cdot \\ E_n \end{bmatrix} \quad [3]$$

The values of J on the left-hand side of this equation are the source terms. They represent the known excitations. The elements of the Y -matrix are functions of the analyzed problem geometry and the boundary constraints. Since each element only interacts with elements in its own neighborhood, the Y -matrix is sparse. The terms of the vector on the right side represent the unknown electric field at each node. These values are obtained by solving the system of linear equations. In order to have a unique solution; it is necessary to constrain the field strength at all boundary nodes.

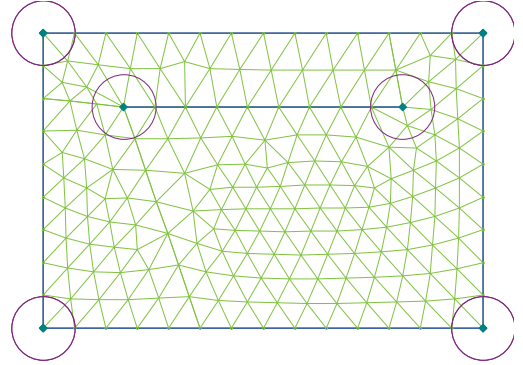


Figure 1. FEM Model

Applied mesh is shown in Figure 1 and the field values at the nodes have been calculated. In each finite element, a linear variation of the field quantity is assumed. The corners of the elements are called *nodes*. The goal is to find the electric field values at these nodes. Other parameters, such as the magnetic field, induced currents, and power loss can be obtained from the electric field values. The modelling was performed with QuickField v5.4.

The characteristics of GTEM-cell [9] are: 50 Ω input impedance, inner conductor at 3/4 height, inner height to width ratio equals 2/3 and angle septum/bottom plate is 15°, with angle septum/top plate being 5°. The septum as well as coating is made of copper. The N type connector is placed at the end of the tapered section. If necessary, the connector can be replaced. The septum is supported by dielectric material. At the other end, there are the pyramidal absorbers 0.25 m long, used for electromagnetic wave termination and two parallel 100 Ω , distributed resistive load for current termination. Figure 2 shows cross-section of the used GTEM-cell.

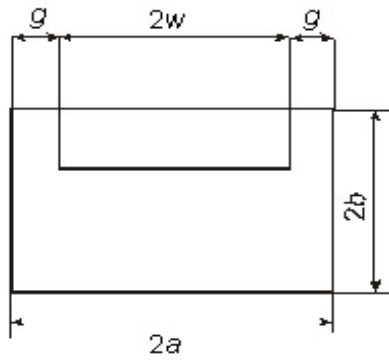


Figure 2. GTEM-cell designed at FER

4. RESULTS

We have modelled a GTEM cell, 40cm high and 60cm wide at cross section. The septum is placed at $\frac{3}{4}$ of height. By changing source values we wanted to see what is the electric field level that would cause temperature to be increased by one 1°C (1K) in the area below the septum, where usually the EUT is placed. Starting temperature in all cases was chosen to be 300 K. Fig.3 and 5 show the result of numerical modelling analysis of E -strength and Figures 4 and 6 show the results of temperature distribution in cell due to E field. Warmer colours in figures indicate higher values of the E field as well as of temperatures.

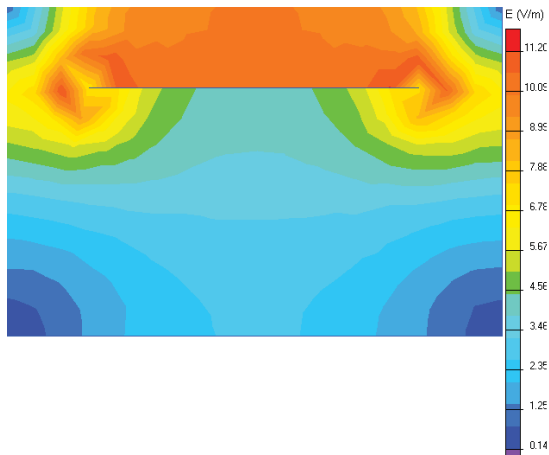


Figure 3. E field distribution for low fields (3.28 V/m below the septum)

Low E -field below the septum, of about 3.28 V/m will increase the temperature by only 0.003 K as shown in Figure 4, while higher E -field of 23 V/m will have a larger effect, increasing the temperature by 0.144 K, as shown in Figures 6-7.

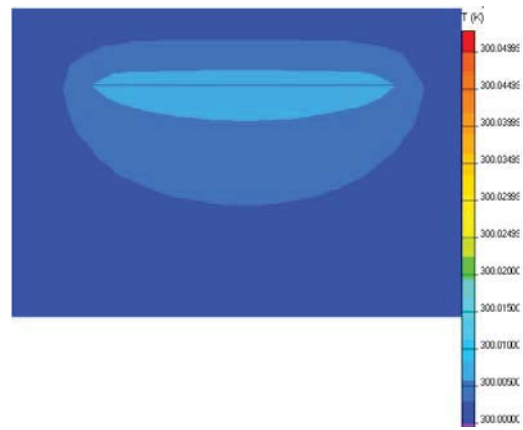


Figure 4. Temperature distribution with low E -field ($\Delta T = 0.003\text{ K}$)

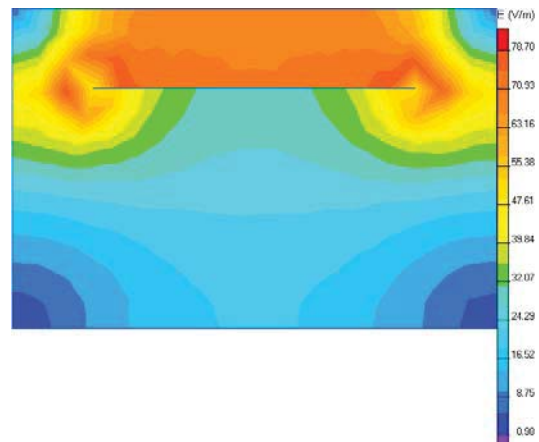


Figure 5. E field distribution for higher fields (23V/m below septum)

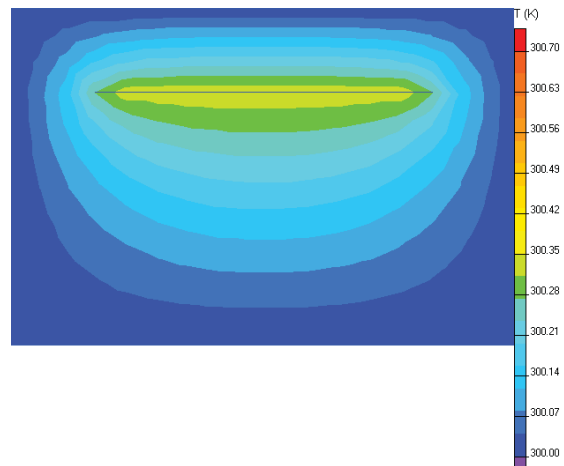


Figure 6. Temperature distribution with higher level E field ($\Delta T = 0.144\text{ K}$)

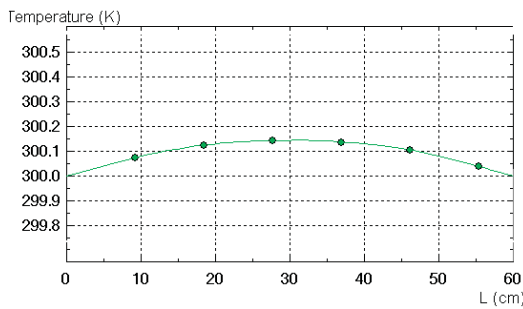


Figure 7. Temperature distribution at 1/2 septum height with $E = 23$ V/m

The temperature is higher just below the septum that is closer to the borders (Fig.7), similar to electric field.

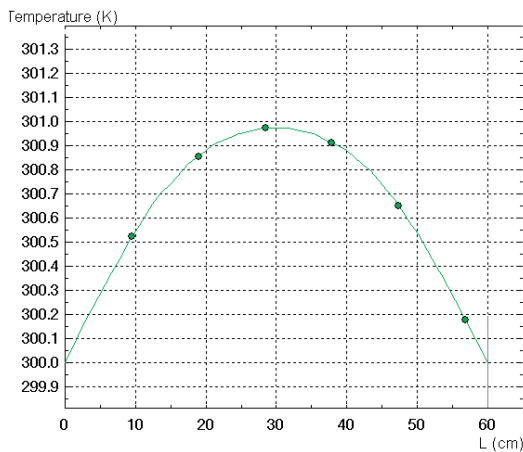


Figure 8. Temperature distribution at 1/2 septum height with $E = 60$ V/m

Table 1. E field in the middle 15 cm below the septum

E level at 1/2 septum height (V/m)	Power density at 1/2 septum height mW/cm^2	$\Delta T (T - T_0)$ K, at 1/2 septum height $T_0=300$ K
3.28	0.0028	0.003
23	0.1403	0.144
60.1	0.9789	0.994

The final model was made for the $\Delta T = 1\text{K}$. The required E field level was approximately 60 V/m at 1/2 septum height. Table I shows the summary results for the models.

5. CONCLUSION

The low E field level (3,3 V/m) should not cause any significant change of the temperature (0.003 K rise). For higher E field level at 1/2 septum height, that is, 23 V/m (Fig. 5,6,7), temperature rise is 0.144 K. It is close to the measured value of 0.1 K [10] at the same E field level. There is no thermal effect for this E -field level. The temperature distribution shows that the largest rise is to

be expected below the septum, and less closer to the boundaries.

Finally, our results show that the E -field level of 60 V/m would increase the temperature by 1 K (1°C). In this case, there would be a thermal effect and the possible biological effects would come from heating rather than from electromagnetic field itself.

6. REFERENCES

- [1] Narda Safety Test Solutions, www.narda-sts.com
- [2] <http://www.arpana.gov.au/mp11.htm>
- [3] International Commission on Non-Ionizing Radiation Protection, www.icnirp.org
- [4] World Health Organization (WHO), EMF-project, www.who.int/peh-emf/
- [5] http://www.deas.harvard.edu/courses/es96/spring1997/web_page/health/thermreg.htm#responses
- [6] Michaelson and Lin: "Biological Effects and Health Implications of RF Radiation", Plenum Press, New York, 1987
- [7] Specific Absorption Rate (SAR) requirements and regulations in different regions, 3rd Generation Partnership Project, 1999
- [8] http://en.wikipedia.org/wiki/Finite_element_analysis
- [9] Kresimir Malaric, Juraj Bartolic, Borivoj Modlic, Absorber and resistor contribution in the GTEM-cell, 2000 IEEE International Symposium on Electromagnetic Compatibility, proceedings Volume 2, 21-25 August, 2000, Washington, D.C., USA, pp. 891-896
- [10] Mirta Tkalec, Kresimir Malaric, Branka Pevalek-Kozlina, Influence of 44, 900 and 1900 MHz Electromagnetic fields on Lemna minor Growth and Peroxidase Activity, Bioelectromagnetics 26:185-193, 2005

Contact:

Prof.dr.sc. Krešimir Malarić
Faculty of Electrical Engineering and Computing (FER)
10000 Zagreb, Croatia
Phone:385 1 6129 650

e-mail: kresimir.malaric@fer.hr
marija.salovarda@dekod.hr